AIP | Applied Physics Letters

Iron on GaN(0001) pseudo-1×1 (1 + 1 12) investigated by scanning tunneling microscopy and first-principles theory

Wenzhi Lin, Andrada-Oana Mandru, Arthur R. Smith, Noboru Takeuchi, and Hamad A. H. Al-Brithen

Citation: Applied Physics Letters **104**, 171607 (2014); doi: 10.1063/1.4874607
View online: http://dx.doi.org/10.1063/1.4874607
View Table of Contents: http://scitation.aip.org/content/aip/journal/apl/104/17?ver=pdfcov
Published by the AIP Publishing

Articles you may be interested in
Growth of high quality N-polar AlN (000 1 ¯) on Si(111) by plasma assisted molecular beam epitaxy
Appl. Phys. Lett. **94**, 151906 (2009); 10.1063/1.3118593

Atomic layer structure of manganese atoms on wurtzite gallium nitride (000 1 ¯)
Appl. Phys. Lett. **93**, 181908 (2008); 10.1063/1.3006434

On the quality of molecular-beam epitaxy grown Fe Mg O and Co Mg O (001) interfaces
J. Appl. Phys. **99**, 08D301 (2006); 10.1063/1.2165914

Spin reorientation transition in ultrathin Co film on In P (2 × 4) reconstructed surface
J. Appl. Phys. **97**, 10J114 (2005); 10.1063/1.1853873

CoSi 2 surface phase separation into self-assembled lateral multilayers
Appl. Phys. Lett. **82**, 1185 (2003); 10.1063/1.1556169

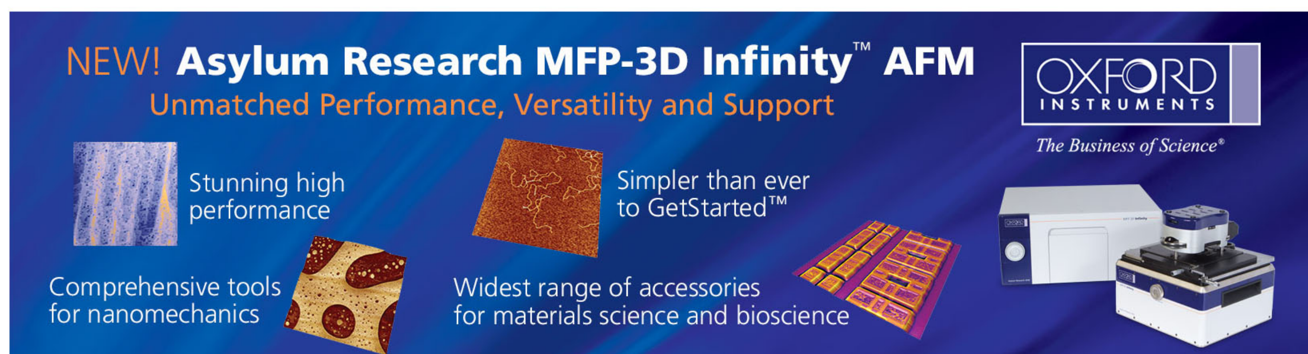

This article is copyrighted as indicated in the article. Reuse of AIP content is subject to the terms at: http://scitation.aip.org/termsconditions. Downloaded to IP: 132.235.26.196 On: Fri, 02 May 2014 19:02:38

APPLIED PHYSICS LETTERS **104**, 171607 (2014)

Iron on GaN(0001) pseudo-1×1 $(1+\frac{1}{12})$ investigated by scanning tunneling microscopy and first-principles theory

Wenzhi Lin,[1] Andrada-Oana Mandru,[1] Arthur R. Smith,[1,a)] Noboru Takeuchi,[2] and Hamad A. H. Al-Brithen[3]

[1]*Department of Physics and Astronomy, Nanoscale and Quantum Phenomena Institute, Ohio University, Athens, Ohio 45701, USA*

[2]*Centro de Nanociencias y Nanotecnologia, Universidad Nacional Autonoma de Mexico Apartado Postal 14, Ensenada Baja California, Codigo Postal 22800, Mexico*

[3]*Physics and Astronomy Department, King Abdulah Institute for Nanotechnology, King Saud University, Riyadh, Saudi Arabia, & National Center for Nano Technology, KACST, Riyadh, Saudi Arabia*

(Received 4 April 2014; accepted 21 April 2014; published online 1 May 2014)

We have investigated sub-monolayer iron deposition on atomically smooth GaN(0001) pseudo-1×1 $(1+\frac{1}{12})$. The iron is deposited at a substrate temperature of 360 °C, upon which reflection high energy electron diffraction shows a transformation to a $\sqrt{3} \times \sqrt{3}$-R30° pattern. After cooling to room temperature, the pattern transforms to a 6×6, and scanning tunneling microscopy reveals 6×6 reconstructed regions decorating the GaN step edges. First-principles theoretical calculations have been carried out for a range of possible structural models, one of the best being a Ga dimer model consisting of 2/9 monolayer of Fe incorporated into 7/3 monolayer of Ga in a relaxed but distorted structure. © *2014 AIP Publishing LLC*. [http://dx.doi.org/10.1063/1.4874607]

Injection of spin-polarized current from ferromagnetic metals into semiconductors is an important approach to enable the use of spin degrees of freedom in semiconductors.[1,2] Efficient spin injection can be achieved using a Schottky tunnel barrier at the metal/semiconductor interface.[3–6] There have been many studies of Fe on conventional semiconductor substrates, including GaAs.[7–13] Recent studies have confirmed that composition and bonding at the Fe/GaAs interface affect spin injection more than bulk properties of the Fe contact.[14]

GaN has found important applications in electronic and optoelectronic devices.[15–17] As a spintronic material, the spin lifetime in pure GaN has been predicted to be about three orders of magnitude larger than that in GaAs.[18] So naturally, there has been great interest in Fe as a spin injector into GaN. Several groups have reported studies of Fe on Ga-polar wurtzite GaN grown by molecular beam epitaxy (MBE).[19–22] A few studies were focused on looking at the initial phase of growth, especially sub-monolayer (sub-ML) Fe deposition.[22,23] He *et al*. reported scanning tunneling microscopy (STM) studies of ultra-thin layers of Fe on bulk-terminated GaN(0001) 1×1 and on GaN(0001) pseudo-1×1, and in the latter case an Fe-induced [0.16 ML Fe] $\sqrt{7} \times \sqrt{7}$ reconstruction was observed.

González-Hernández *et al*. recently reported a first-principles density functional theory study of sub-ML Fe atom coverages on both a bulk-terminated GaN(0001) surface using a 2×2 unit cell, and on a Ga double-layer-terminated (sometimes referred to as Ga bi-layer) GaN(0001) (pseudo-1×1) surface using a $\sqrt{3} \times \sqrt{3}$ unit cell.[24] For the latter case, Fe incorporation within the Ga double-layer was found to be energetically unfavorable, becoming more unfavorable with increasing Fe concentration. However, Ga rich growth conditions leading to the Ga double-layer surface are well known to give best overall GaN material quality for devices.[25–29] Therefore, it is important to explore what kind of Fe-containing structures, if any, can be stabilized on the pseudo-1×1 surface.

Here, we report a study of the initial phase of Fe growth on atomically smooth GaN(0001) pseudo-1×1, in particular the pseudo-1×1 $(1+\frac{1}{12})$ surface (hereafter referred to just as $1+\frac{1}{12}$). Although the GaN(0001) pseudo-1×1 consists of a double layer of Ga on top of the last GaN bilayer,[30] few studies have distinguished between the $1+\frac{1}{12}$ and the pseudo-1×1 $(1+\frac{1}{6})$ surface (hereafter just $1+\frac{1}{6}$) as the starting substrate surface. However, it is known that the $1+\frac{1}{12}$ surface is more Ga-rich than the $1+\frac{1}{6}$ surface.[30] Here, we find that the $1+\frac{1}{12}$ surface is critical to the successful formation of the Fe-containing Ga double layer. We combine the experimental results with first-principles theoretical calculations to understand the Fe-containing structure including the effect of Ga adatoms displaced by Fe atom incorporation.

We performed the experiments in a custom-designed MBE/STM system. The MBE chamber includes Fe and Ga effusion cells and a radio-frequency (rf) N plasma source. Iron and Ga fluxes are calibrated using a quartz crystal thickness monitor. The N flux is set by controlling the growth chamber pressure and plasma source power. The surface is monitored during growth using reflection high energy electron diffraction (RHEED).

After cleaning with solvents, a GaN(0001)/Al_2O_3 substrate was heated at ~720 °C under N plasma for 20–30 min. GaN growth was carried out with the sample at ~680 °C, with Ga flux ~4.8×10^{14}/cm^{2}s, growth chamber pressure set to ~2.1×10^{-5} Torr. After a smooth surface was established, the sample was cooled to room temperature (RT) to verify the existence of $1+\frac{1}{12}$ structure. Iron was subsequently deposited with the substrate set to ~360 °C and using a nominal Fe deposition rate of $1.1 \pm 0.4 \times 10^{13}$ atoms/cm^{2}s. For the sample used for the STM images

a)E-mail: smitha2@ohio.edu

 © 2014 AIP Publishing LLC

This article is copyrighted as indicated in the article. Reuse of AIP content is subject to the terms at: http://scitation.aip.org/termsconditions. Downloaded to IP: 132.235.26.196 On: Fri, 02 May 2014 19:02:38

presented here, the intended amount deposited was $3.4 \pm 1.4 \times 10^{14}$ atoms/cm$^2 = 0.30 \pm 0.12$ ML [based on the GaN(0001) lattice having a density of $\sim 11.4 \times 10^{14}$ atoms/cm$^2 \equiv 1$ ML]. For a second sample having an intended deposition of 0.52 ± 0.21 ML, Auger electron spectroscopy (AES) was performed in order to assess the chemical content. STM and AES experiments were both performed at RT after transferring the sample directly from the MBE chamber into the UHV analysis chamber.

The RHEED patterns before Fe deposition are shown in Figs. 1(a) and 1(b) at RT (25 °C) and Figs. 1(c) and 1(d) at the growth temperature, indicating an atomically smooth GaN(0001) $1+\frac{1}{12}$ surface. The streaky RHEED patterns after sub-ML Fe deposition, shown in Figs. 1(e) and 1(f) at 360 °C and Figs. 1(g) and 1(h) at RT, show that a smooth and well-ordered Fe-containing surface is produced. We see that, at the growth temperature, $\frac{1}{3}$- and $\frac{2}{3}$-order streaks appear in the RHEED pattern along $\langle 1\bar{1}00\rangle$, suggesting a $\sqrt{3} \times \sqrt{3}$ - R30° structure. Then, after cooling to RT, the RHEED pattern further develops as $\frac{1}{6}$-order streaks appear along both azimuths.

Shown in Fig. 2 is a filled-states STM image ($V_S = -1.75$ V) of the $1+\frac{1}{12}$ surface after Fe deposition taken at RT. Clearly observed is the formation of 2-dimensional and hexagonally reconstructed regions adhered to the step edges of the $1+\frac{1}{12}$ surface. The 6×6 regions appear as raised, reconstructed areas typified by an array of hexagonally located depressions (dark sites). The in-between areas appear featureless, as typical of the pseudo-1×1 surface. In one location, a 6×6 vacancy island is seen. We also find the 6×6-structure regions around the spiral dislocation centers at the leading edges of the spiral growth fronts. Here, the topography varies in a curving manner but does not affect the 6×6 growth. Also to be noted are the existence of both single height (2.59 Å) and double height (5.19 Å) GaN bi-layer steps, along both of which are found the same 6×6 regions. For comparison, shown in Fig. 3(a) is an STM image of just the $1+\frac{1}{12}$ surface at RT before Fe deposition, revealing atomically smooth and featureless terraces separated also by both single and double-height GaN bi-layer steps.

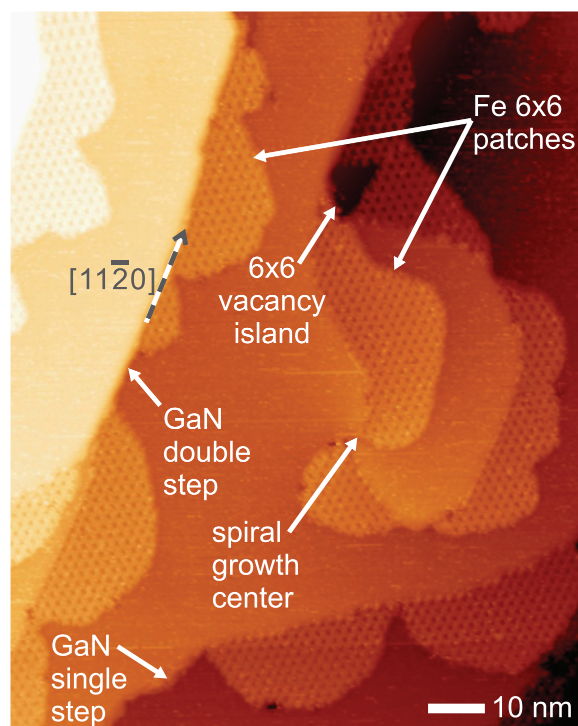

FIG. 2. STM image of the Fe/GaN $1+\frac{1}{12}$ surface showing hexagonal-like regions adjacent to GaN single and double height steps, including also two steps emerging from a spiral growth center located around a screw-type dislocation. Sample bias $V_S = -1.75$ V, tunnel current $I_T = 0.10$ nA.

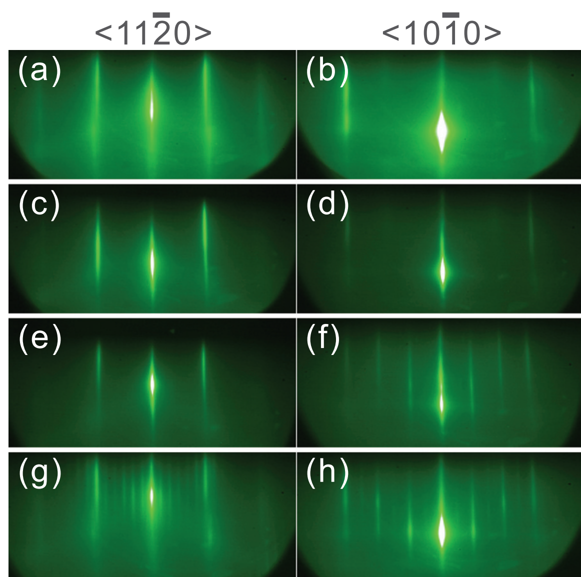

FIG. 1. RHEED patterns for Fe on GaN(0001) $1+\frac{1}{12}$ taken along GaN $\langle 11\bar{2}0\rangle$ (left) and $\langle 10\bar{1}0\rangle$ (right). [(a) and (b)] the MBE-grown GaN surface at RT; [(c)/(d)] the MBE-grown GaN surface at HT (360 °C); [(e)/(f)] the surface after Fe deposition at HT; [(g)/(h)] the surface after Fe deposition at RT.

The size of the hexagonal unit cell, as also suggested by the $\frac{1}{6}$-order RHEED streaks at RT, is 6×6, whereas the total size of the hexagonal 6×6 regions varies from a few unit cells (several nm wide) up to over a hundred unit cells (tens of nm wide). They are adhered randomly along the step edges as also shown in Fig. 3(b) and typically do not cover the entire terrace, leaving areas of just pseudo-1×1 like that shown in Fig. 3(a). While some of the hexagonal regions have curving shapes, some others suggest a V-shape indicating preferential growth along certain crystal directions. We do not find that any of the 6×6 regions nucleate at the centers of the terraces.

Shown in the inset to Fig. 3(b) is a high resolution, filled-states STM image of a 6×6 region. It shows that the 6×6 is marked by an array of both protrusions and depressions on a 6×6 hexagonal lattice. The height and corrugations of the reconstruction are shown in Fig. 3(c); as seen, the 6×6 domains are ~ 1.8 Å above the level of the pseudo-1×1 terrace, irrespective of whether it is a single- or double-height GaN step. The corrugation amplitude measures quite large, 0.6–0.8 Å peak-to-valley.

One must consider that at the Fe deposition temperature (~ 360 °C), the $1+\frac{1}{12}$ surface is in a highly fluidic state, the double Ga layer being liquid-like. Iron is deposited into this fluidic Ga sea. So rather than the picture of island nucleation on an already-stable substrate surface as common in many well-known systems, the picture here is one of Fe atoms

This article is copyrighted as indicated in the article. Reuse of AIP content is subject to the terms at: http://scitation.aip.org/termsconditions. Downloaded to IP: 132.235.26.196 On: Fri, 02 May 2014 19:02:38

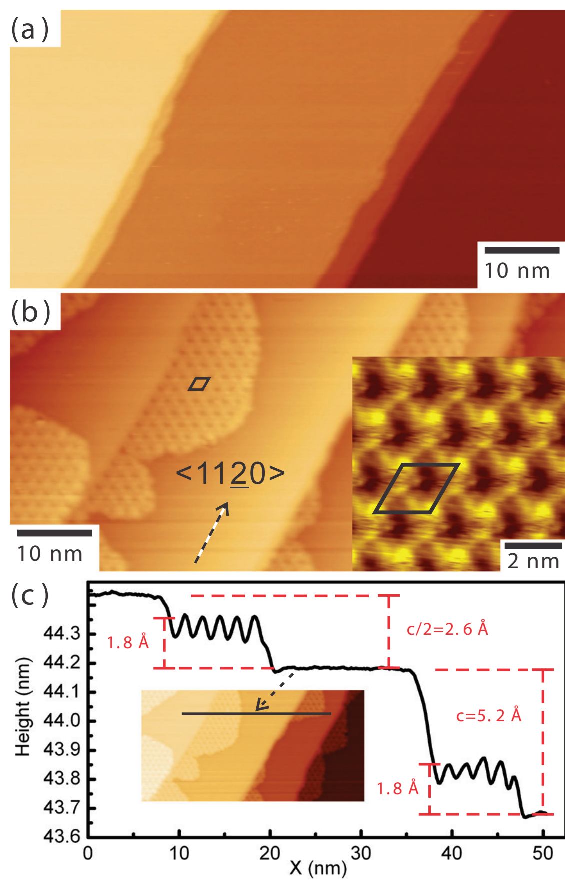

FIG. 3. (a) STM image of GaN(0001) $1+\frac{1}{12}$ surface before Fe deposition; (b) STM image of 6×6 hexagonal-like regions adjacent to GaN steps, $V_S=-1.75$ V, $I_T=0.10$ nA for both (a) and (b); inset to (b): high resolution STM image of Fe/GaN structure with 6×6 unit cell, $V_S=-1.50$ V, $I_T=0.14$ nA; (c) Line profile across the step structures at the location indicated by the inset to (c).

somehow inducing an ordered structure (i.e., a $\sqrt{3}\times\sqrt{3}$-R30°) at high temperature (HT), while Ga adatoms are released and continue to move freely in other parts of the surface. Then the ordered regions themselves may become the precursors of the stable 6×6 structures seen in STM at RT.

One possibility for the structure of the $\sqrt{3}\times\sqrt{3}$-R30° regions at HT is the formation of a $\sqrt{3}\times\sqrt{3}$-R30° structure consisting of 1 Fe atom per unit cell; this would be a 1/3 ML Fe model. However, this kind of model was found to be unstable by Gonz*á*lez-Hern*á*ndez *et al*. as noted above, and in our work as well. This is as opposed to the case of manganese, where sub-ML Mn deposition on the $1+\frac{1}{6}$ surface forms very stable stripe-like $\sqrt{3}\times\sqrt{3}$-R30° structures both at the Mn deposition temperature (~250 °C), and at RT.[31] Therefore, for the Fe case, other HT models must be considered.

Upon cooling, Ga atoms displaced by Fe atoms will become less energetic, and then the ordered $\sqrt{3}\times\sqrt{3}$-R30° regions will form the basis of a substrate on which the excess Ga atoms can condense. A line profile measurement is taken across two GaN steps and two 6×6 regions, as presented in Fig. 3(c). One step is a single bilayer GaN step, while the lower step is a double GaN bilayer step. In all cases, the $6\times$ regions have the same surface periodicity ($6a$) and the same z-height which measures ~1.8 Å relative to the $1+\frac{1}{12}$ terrace.

Theoretical calculations were performed in the framework of periodic density functional theory as implemented in the PWscf (plane waves-self-consistent-field) code,[32] treating the exchange and correlation potential energies according to the generalized gradient approximation (GGA). We have used Vanderbilt ultra-soft pseudopotentials,[33] along with $(4\times4\times1)$ and $(2\times2\times1)$ Monkhorst-Pack meshes to sample the Brillouin zone for the $\sqrt{3}\times\sqrt{3}$-R30° and 3×3 geometries, respectively. Kinetic energy cutoffs of 30 and 240 Ry were used, to represent the wave function and charge density.

The calculations have been carried out employing the repeated slab geometry, each slab consisting of 4 GaN bilayers + a double layer of Ga atoms representing the pseudo-1×1 structure. The Fe atoms are included within the top Ga layer. The bottom surface was saturated by fractional pseudo hydrogen atoms. Consecutive slabs were separated by an empty space ~10.0 Å wide. The three topmost GaN bilayers, the double Ga layer, and the Fe atoms had full freedom to move. The bottom GaN bilayer and the saturating pseudo H atoms were frozen in order to simulate a bulk-like environment. The energy of the ideal GaN bilayer-terminated surface is taken as the zero energy reference point [see Fig. 5 where the surface formation energy is given in eV/(1×1) cell].

Shown in Figs. 4(a) and 4(b) are the side and top views, respectively, of the *in-plane* $\sqrt{3}\times\sqrt{3}$-R30° structure having one substitutional Fe atom per $\sqrt{3}\times\sqrt{3}$-R30° unit cell; this

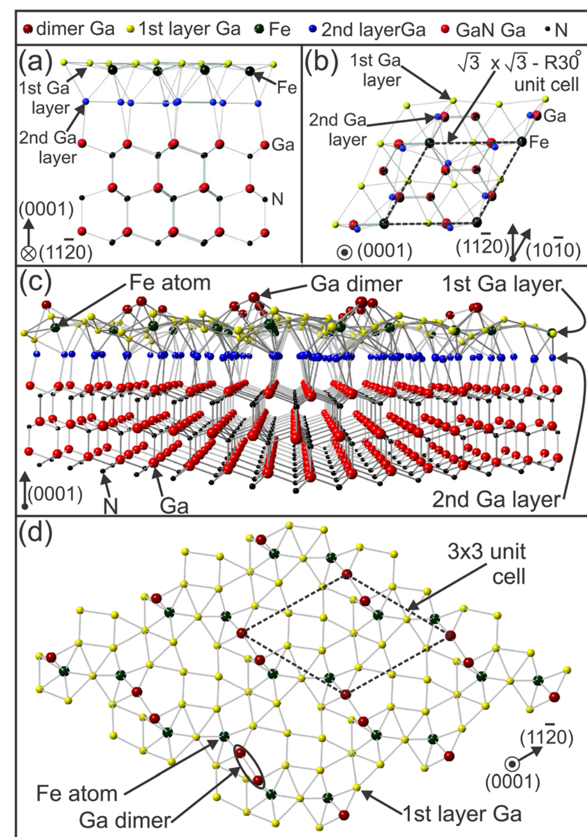

FIG. 4. (a) side view and (b) top view of the flat (*in-plane*) $\sqrt{3}\times\sqrt{3}$-R30° (unstable) structure; (c) perspective view of the 2/9 ML Fe + 7/3 ML Ga dimer model showing all atoms including 3 GaN layers; (d) top view of the 2/9 ML Fe + 7/3 ML Ga dimer model showing only the top highly distorted Fe+Ga layer.

This article is copyrighted as indicated in the article. Reuse of AIP content is subject to the terms at: http://scitation.aip.org/termsconditions. Downloaded to IP: 132.235.26.196 On: Fri, 02 May 2014 19:02:38

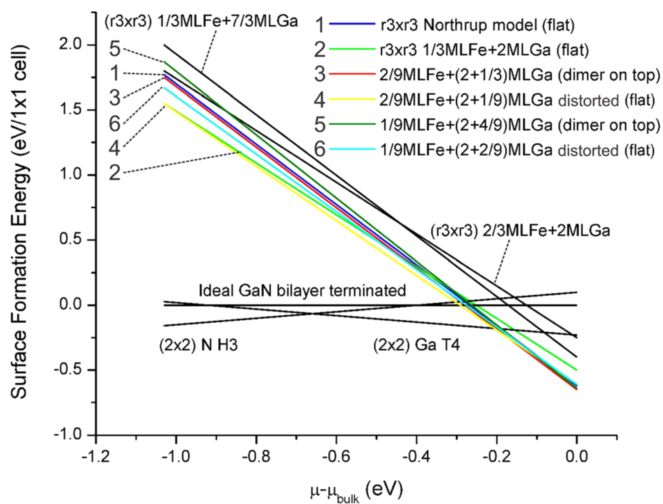

FIG. 5. Surface formation energy as a function of Ga chemical potential relative to bulk Ga for various Fe/GaN(0001) pseudo-1×1 models. Model 1 is the Northrup Ga $\sqrt{3} \times \sqrt{3}$-R30° pseudo-1×1 model. The zero energy reference is set by the ideal GaN terminated bi-layer model.

model (referred to as a "flat" model) is the most stable configuration of the $\sqrt{3} \times \sqrt{3}$-R30° structure as calculated in the $\sqrt{3} \times \sqrt{3}$ geometry. However, the flat model is unstable with respect to the $\sqrt{3} \times \sqrt{3}$-R30° Northrup model for the pseudo-1×1,[34] as can be seen by inspecting Fig. 5 (model 2 vs. model 1), and in agreement with the findings of Gonzalez-Hernandez *et al.*[24]

After expanding the calculation to a 3×3 cell, however, the flat model becomes metastable, relaxing to a model *not* having $\sqrt{3} \times \sqrt{3}$-R30° periodicity. A somewhat lower energy model (see model 4, Fig. 5) is obtained by replacing one out of the 3 Fe's in the 3×3 cell with a Ga atom, leading to the 2/9 ML Fe + 2 + 1/9 ML Ga distorted (flat) model. A better model energetically is obtained after adding an additional $\frac{2}{9}$ ML Ga to this surface, resulting in the 2/9 ML Fe + 7/3 ML Ga (dimer on top) model which includes one Ga dimer per each 3×3 cell, as presented in Figs. 4(c) and 4(d), and Fig. 5 (model 3). However, two competing models (models 5 and 6 in Fig. 5) to this one (model 3), each containing only 1/9 ML Fe, are energetically almost the same [within 0.01 eV/(1×1)] at high Ga chemical potentials.

Referring back to the RHEED patterns shown in Figs. 1(g) and 1(h), it is seen that along $\langle 11\bar{2}0 \rangle$ the 6× streaks are quite uniform in intensity, whereas along $\langle 1\bar{1}00 \rangle$ their intensity is uneven. Therefore, it confirms the fairly complicated 6×6 structure suggested by the model and by the high resolution STM image of the 6×6 shown in the inset of Fig. 3(b).

The dimer model shows significant *in-plane* as well as *out-of-plane* relaxation and distortion. Clearly, the Ga dimers are very pronounced topographically on the surface as seen in the perspective view [Fig. 4(c)]. It may therefore be expected that such lifted-up dimer features as well as intervening (i.e., *valley*) regions could form the basis of a hexagonally corrugated 6×6 structure.

We see that the formation energy for the 2/9 ML Fe + 7/3 ML Ga (dimer on top) model (model 3), as shown in Fig. 5, is very slightly lower than that for the Northrup $\sqrt{3} \times \sqrt{3}$-R30° pseudo-1×1 model (model 1). This slight energetic advantage could stabilize its structure, but only a slight advantage over the Northrup Ga model effectively means that it may be difficult for Fe to stick to the pseudo-1×1 surface. And that indeed is what is found in the experiment. If we assume the 2/9 ML Fe content of the Ga dimer model for the 6×6 regions, and with a measured 28% of the surface being covered by 6×6 regions for the sample imaged in Fig. 2, the weighted average coverage for the whole surface is 0.062 ML (=0.22 ML × 0.28); this is assuming no Fe within the non-6×6 regions. Given the intended deposition was 0.30 ± 0.12 ML, this gives a sticking coefficient S of 0.21 ± 0.08.

To verify the surface stoichiometry, we measured a second sample using AES, in which the intended deposition $(0.52 \pm 0.21 \text{ ML}) \times S$ gives an expected average coverage of 0.11 ± 0.08 ML. For this surface, the AES Fe:Ga ratio was measured to be in the range 2.5%–6.5% [determined as (I_{Fe}/S_{Fe}):(I_{Ga}/S_{Ga}), where I_{Fe} (I_{Ga}) is the derivative mode peak-peak intensity for Fe (Ga) and S_{Fe} (S_{Ga}) is the sensitivity factor for Fe (Ga) as determined by calibrating our AES spectrometer with standard samples]. This AES Fe:Ga ratio is very reasonable given the large amount of Ga contained in the pseudo-1×1 structure. Assuming an average Fe coverage for the surface of 0.064 ML (based on the 6×6 areal fraction measured by STM (29%) multiplied by the 2/9 ML Fe content of model 3 or 4), we calculate an expected value for the Fe:Ga AES ratio of 3.4%, in excellent agreement with the measured AES ratio. On the other hand, if we assume an average Fe coverage based on the 1/9 ML models (models 5 and 6), we calculated an expected Fe:Ga AES ratio of only 1.7%, in slightly less good agreement with the measured AES values.

The results presented here form the following picture. At the Fe deposition temperature (360 °C), a small amount of deposited Fe (say < 1/3 ML) concentrating into localized areas of the top Ga layer stabilizes a $\sqrt{3} \times \sqrt{3}$-R30° structure. This could be a Northrup-type pseudo-1×1 structure stabilized by Fe impurities. Meanwhile at HT, additional (or displaced) Ga atoms move freely on the surface. As the structure cools down to RT, the free Ga adatoms condense onto the stabilized Fe-containing regions, leading to a relaxed and highly distorted dimer-like structure with large unit cell as observed.

In conclusion, the results suggest that Fe incorporates within the top Ga layer of the GaN(0001) $1 + \frac{1}{12}$ surface at HT, displacing Ga's which then become adatoms and/or Ga dimers. As cooling occurs, condensation of these Ga adatoms plays a strong role in leading to the formation of the RT 6×6 structure which is found along the GaN step edges. The first-principles calculations using 3×3 cells show that a relaxed and highly distorted Ga dimer structure containing 1/9 or 2/9 ML Fe in the top layer is slightly better, energetically than the Northrup Ga $\sqrt{3} \times \sqrt{3}$-R30° pseudo-1×1 model in the Ga-rich limit. Future work could entail more extended theoretical calculations in a full 6×6 cell geometry. Of greater interest, however, would be to look into the possible magnetic properties of the 6×6 structure.

This work has been supported by the U.S. Department of Energy, Office of Basic Energy Sciences (Grant No. DE-FG02-06ER46317). The computations were performed in the

This article is copyrighted as indicated in the article. Reuse of AIP content is subject to the terms at: http://scitation.aip.org/termsconditions. Downloaded to IP: 132.235.26.196 On: Fri, 02 May 2014 19:02:38

DGSCA-UNAM supercomputing center. N.T. acknowledges support by DGAPA-UNAM (Grant No. IN101809) and CONACYT (Grant No. 164485). WSxM is acknowledged for image processing.[35]

[1]S. A. Wolf, D. D. Awschalom, R. A. Buhrman, J. M. Daughton, S. von Molnár, M. L. Roukes, A. Y. Chtchelkanova, and D. M. Treger, Science **294**, 1488 (2001).
[2]P. Sharma, Science **307**, 531 (2005).
[3]A. T. Hanbicki, B. T. Jonker, G. Itskos, G. Kioseoglou, and A. Petrou, Appl. Phys. Lett. **80**, 1240 (2002).
[4]A. T. Hanbicki, O. M. J. van 't Erve, R. Magno, G. Kioseoglou, C. H. Li, B. T. Jonker, G. Itskos, R. Mallory, M. Yasar, and A. Petrou, Appl. Phys. Lett. **82**, 4092 (2003).
[5]A. T. Hanbicki, G. Kioseoglou, M. A. Holub, O. M. J. van't Erve, and B. T. Jonker, Appl. Phys. Lett. **94**, 082507 (2009).
[6]C. Adelmann, X. Lou, J. Strand, C. Palmstrøm, and P. A. Crowell, Phys. Rev. B **71**, 121301 (2005).
[7]A. Filipe, A. Schuhl, and P. Galtier, Appl. Phys. Lett. **70**, 129 (1997).
[8]L. Winking, M. Wenderoth, J. Homoth, S. Siewers, and R. G. Ulbrich, Appl. Phys. Lett. **92**, 193102 (2008).
[9]B. R. Cuenya, A. Naitabdi, E. Schuster, R. Peters, M. Doi, and W. Keune, Phys. Rev. B **76**, 094403 (2007).
[10]F. Monteverde, A. Michel, J.-P. Eymery, and P. Guérin, J. Cryst. Growth **267**, 231 (2004).
[11]S. Mirbt, B. Sanyal, C. Isheden, and B. Johansson, Phys. Rev. B **67**, 155421 (2003).
[12]M. Doi, B. R. Cuenya, W. Keune, T. Schmitte, A. Nefedov, H. Zabel, D. Spoddig, R. Meckenstock, and J. Pelzl, J. Magn. Magn. Mater. **240**, 407 (2002).
[13]C. Godde, S. Noor, C. Urban, and U. Köhler, Surf. Sci. **602**, 3343 (2008).
[14]B. D. Schultz, N. Marom, D. Naveh, X. Lou, C. Adelmann, J. Strand, P. A. Crowell, L. Kronik, and C. J. Palmstrøm, Phys. Rev. B **80**, 201309 (2009).
[15]H. W. Choi, C. Liu, E. Gu, G. McConnell, J. M. Girkin, I. M. Watson, and M. D. Dawson, Appl. Phys. Lett. **84**, 2253 (2004).
[16]S. J. Pearton and F. Ren, Adv. Mater. **12**, 1571 (2000).
[17]C.-F. Chu, C.-C. Cheng, W.-H. Liu, J.-Y. Chu, F.-H. Fan, H.-C. Cheng, T. Doan, and C. A. Tran, Proc. IEEE **98**, 1197 (2010).
[18]S. Krishnamurthy, M. van Schilfgaarde, and N. Newman, Appl. Phys. Lett. **83**, 1761 (2003).
[19]R. Calarco, R. Meijers, N. Kaluza, V. A. Guzenko, N. Thillosen, T. Schäpers, H. Lüth, M. Fonin, S. Krzyk, R. Ghadimi, B. Beschoten, and G. Güntherodt, Phys. Status Solidi A **202**, 754 (2005).
[20]R. Meijers, R. Calarco, N. Kaluza, H. Hardtdegen, M. v. D. Ahe, H. L. Bay, H. Lüth, M. Buchmeier, and D. E. Bürgler, J. Cryst. Growth **283**, 500 (2005).
[21]C. Gao, O. Brandt, H.-P. Schönherr, U. Jahn, J. Herfort, and B. Jenichen, Appl. Phys. Lett. **95**, 111906 (2009).
[22]Y. Honda, S. Hayakawa, S. Hasegawa, and H. Asahi, Appl. Surf. Sci. **256**, 1069 (2009).
[23]K. He, L. Y. Ma, X. C. Ma, J. F. Jia, and Q. K. Xue, Appl. Phys. Lett. **88**, 232503 (2006).
[24]R. González-Hernández, W. López P., M. G. Morena-Armenta, and J. A. Rodríguez, J. Appl. Phys. **109**, 07C102 (2011).
[25]E. J. Tarsa, B. Heying., X. H. Wu, P. Fini, S. P. DenBaars, and J. S. Speck, J. Appl. Phys. **82**, 5472 (1997).
[26]G. Mula, C. Adelmann, S. Moehl, J. Oullier, and B. Daudin, Phys. Rev. B **64**, 195406 (2001).
[27]J. Neugebauer, T. K. Zywietz, M. Scheffler, J. E. Northrup, H. Chen, and R. M. Feenstra, Phys. Rev. Lett. **90**, 056101 (2003).
[28]T. D. Moustakas and A. Bhattacharyya, Phys. Status Solidi **C9**, 580 (2012).
[29]E. Monroy, M. Hamilton, D. Walker, P. Kung, F. J. Sanchez, and M. Razeghi, Appl. Phys. Lett. **74**, 1171 (1999).
[30]A. R. Smith, R. M. Feenstra, D. W. Greve, M. S. Shin, M. Skowronski, J. Neugebauer, and J. E. Northrup, J. Vac. Sci. Technol. B **16**, 2242 (1998).
[31]K. K. Wang, N. Takeuchi, A. Chinchore, W. Lin, Y. Liu, and A. R. Smith, Phys. Rev. B **83**, 165407 (2011).
[32]P. Giannozzi, S. Baroni, N. Bonini, M. Calandra, R. Car, C. Cavazzoni, D. Ceresoli, G. L. Chiarotti, M. Cococcioni, I. Dabo, A. Dal Corso, S. Fabris, G. Fratesi, S. de Gironcoli, R. Gebauer, U. Gerstmann, C. Gougoussis, A. Kokalj, M. Lazzeri, L. Martin-Samos, N. Marzari, F. Mauri, R. Mazzarello, S. Paolini, A. Pasquarello, L. Paulatto, C. Sbraccia, S. Scandolo, G. Sclauzero, A. P. Seitsonen, A. Smogunov, P. Umari, and R. M. Wentzcovitch, J. Phys.: Condens. Matter **21**, 395502 (2009).
[33]D. Vanderbilt, Phys. Rev. B **41**, 7892 (1990).
[34]J. E. Northrup, J. Neugebauer, R. M. Feenstra, and A. R. Smith, Phys. Rev. B **61**, 9932 (2000).
[35]I. Horcas, R. Fernandez, J. M. Gomez-Rodriguez, J. Colchero, J. Gomez-Herrero, and A. M. Baro, Rev. Sci. Instrum. **78**, 013705 (2007).

This article is copyrighted as indicated in the article. Reuse of AIP content is subject to the terms at: http://scitation.aip.org/termsconditions. Downloaded to IP: 132.235.26.196 On: Fri, 02 May 2014 19:02:38